International Journal of Thin Films Science and Technology

http://dx.doi.org/10.18576/ijtfst/150203

Analysis of the Damage Behavior and Mechanical Durability of Zinc Oxide (ZnO) Coatings on Photovoltaic Panel Glass

Ali Ooda Abd[1,2,*], *Anas Bouguecha*[1] *and Mohamed Haddar*[1]

[1] Laboratory of Mechanics Modeling and Production, National Engineering School of Sfax, University of Sfax, Sfax, Tunisia
[2] Department of Applied Physics, College of Applied Sciences, University of Technology, Baghdad, Iraq

Received: 22 Feb. 2026, Revised: 12 Apr. 2026, Accepted: 26 Apr. 2026
Published online: 1 May 2026

Abstract: In this study ZnO thin film (1 µm thickness) were prepared by hydrolysis and deposited by thermal spraying on glass substrates in this study. Erosive wear was evaluated at a constant velocity of 4 m/s for 30 min using a custom-built desert wind and sand erosion simulation system. The experimental design used impingement angles of 15°, 30°, 45° and 60° to map wear mechanisms. The materials were characterized by X-ray diffraction (XRD), UV-VIS spectroscopy, Scanning Electron Microscopy (SEM), Energy Dispersive X-ray (EDX) and Atomic Force Microscopy (AFM). The product was characterized by a fine crystalline structure with a sharper and stronger diffraction peaks with 15.91 nm of crystallite size and high transmittance in the optical spectrum reaching 86%. Relative erosion rate was continuously increased with the impact angle, from 0.00164 mg/g at 15° to 0.00220 mg/g at 60°. This is typical of brittle materials where the degradation process is dominated by the normal impact stresses that cause crack initiation, propagation and spallation. The present study concludes that the ZnO coating exhibited clearly brittle fracture mechanics under sand bombardment. These films are mechanically not stable under high angle impacts but still sufficiently transparent. These results provide basic engineering guidance for the maintenance and long-term operation of photovoltaic plants in erosive desert climates.

Keywords: ZnO Thin Film, Erosion, Impact Angle, Mechanical Durability.

1 Introduction

1.1. Research Background

Solar energy is a major renewable resource. However, the efficiency of photovoltaic (PV) power generation is severely affected by soiling, the accumulation of atmospheric dust [1,2]. In dry environments, this accumulation can reduce power output by as much as 50% within eight months if the panels are not maintained [3]. Thus, the need for effective mitigation strategies such as anti-soiling coatings in order to maintain PV module efficiency in harsh climates is increasing [4,5]. Metal oxide coatings like Zinc Oxide (ZnO) are promising solutions to minimize dust adhesion by making the surfaces hydrophobic [6]. But solid particle erosion from windblown sand degrades these protective layers significantly [9]. It is well known that the impingement angle is a controlling factor in this wear mechanism. Materials behave in a ductile manner with maximum erosion at acute angles, or in a brittle manner with maximum damage at normal incidence (90°) [6-11]. The literature is lacking in this respect, as most of the studies are devoted to the optimization of chemical precursors or surface morphology and not to the specific durability of the coated layer against erosion [12]. Detailed information on the mechanisms of how physical properties influence particle motion and erosion on PV panels is scarce, which is crucial for long-term safe operation [13,14]. Moreover, although other materials such as TiO2 films have been studied, the relationship between erosion angles and the durability of ZnO coatings is still in its infancy [12-15]. This study fills these gaps by investigating the damage behavior of ZnO coatings on the top glass of PV panels. The aim of the study is to evaluate the erosive wear effect on the durability of Zinc Oxide by examining the relationship between the erosion and impact angle. These findings provide important engineering guidance to the sustained efficient operation of PV panels in erosive desert conditions [16,17].

1.2. State of the art.

Recent research has shown that Zinc oxide (ZnO) has become a highly promising multifunctional coating for photovoltaic (PV) modules owing to its wide band gap (>3eV), anti-reflection and self-cleaning properties [1-3]. It has been recently shown that ZnO can be engineered to be super hydrophobic (WCAs > 150°) or super hydrophilic by controlling its crystalline structure into specific nano-morphologies such as nanowires or Nano belts that facilitate the photo catalytic breakdown of organic pollutants [4-6]. To assess the mechanical robustness of these functional thin films, typically solid particle erosion (SPE) tests are performed following ASTM G76. These devices use high-pressure streams of air to propel an abrasive media, such as silica or alumina, against the surface of a target to accurately measure the mass loss and

*Corresponding author E-mail: hamedalwan14@gmail.com

volumetric wear [7-9]. Key challenges and gaps However, there are still some bottlenecks in the practical application of ZnO coatings. Firstly, pure metal oxides are structurally fragile and intrinsically brittle in general. Material removal in these coatings is usually controlled by brittle fracture mechanics, including the intersection of lateral and radial cracks, which leads to considerable mass loss under high-angle impacts [10-12]. Second, the mechanical stability of ZnO thin film is often compromised by granular structures that adhere to surfaces via weak Van der Waals forces, resulting in a high tendency for delamination under harsh mechanical impacts [13-14]. Thirdly, it is a challenge to balance the high surface roughness for super hydrophobicity and the high optical transparency for PV module efficiency [15]. Lastly, the current literature is overly focused on optimizing chemical precursors and photocatalytic performance rather than exploring long-term mechanical resilience [2,16]. This direct evaluation of pure ZnO on an erosion testing device thus bridges the gap between the purely chemical/photocatalytic evaluations and the micro-abrasive wear resistance needed for real-world durability in arid environments [2,17].

2. Materials and experimental Study.

2.1. Practical Part

Using a heated stirrer at 70°C for two hours, 0.81 and 2.33 grams of the material were dissolved in 100 milliliters of non-ionic water to create zinc oxide nanoparticles at a molar concentration of 0.1 M. Following the acquisition of the nanoparticle solution, it was thermally sprayed onto 2.5 x 2.5 cm glass slides to a thickness of about 1 µm, as illustrated in Fig (1). Gravimetric measurement was used to determine the thickness. Five drops of a solution containing 25 microliters of zinc oxide nanoparticles were applied to glass substrates at a temperature of 50°C.

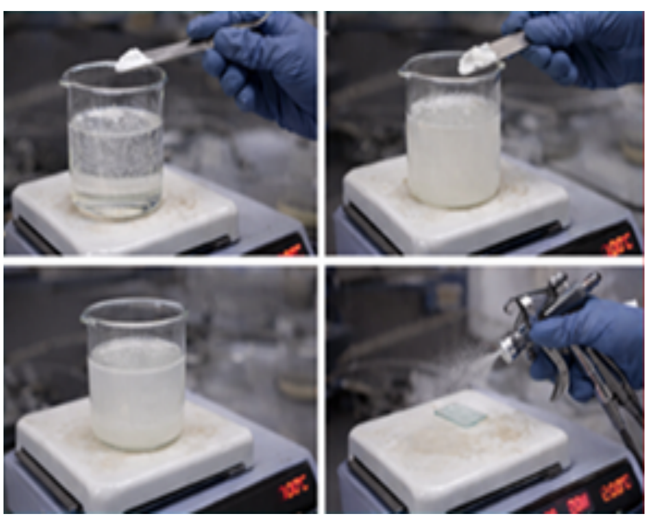

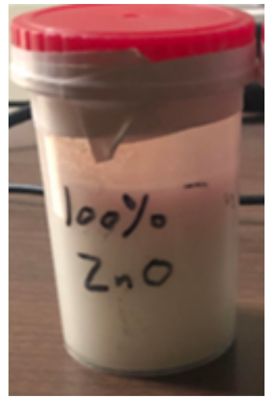

Fig. 1: Nanoparticles of Zinc oxide prepared by hydrolysis.

2.2. Erosion Experiments and Impact Studies.

2.2.1. Experimental Methods and Equipment.

The experimental platform constructed in this section is a desert wind and sand

erosion simulation system, whose structure is shown in Fig (2). [14].

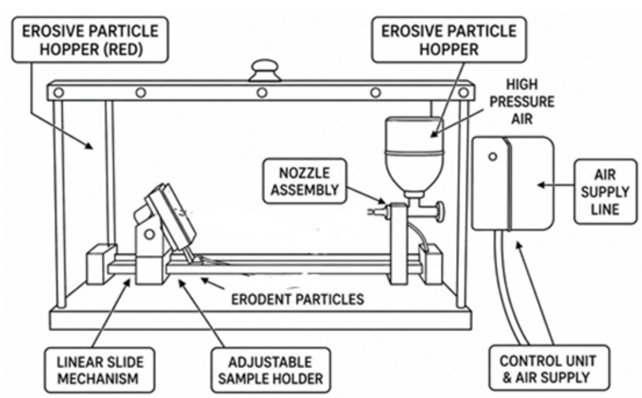

Fig. 2: Desert wind and sand erosion simulation system.

The experimental platform consists of an air compressor, airflow control valves, a sandbox, a sandblasting gun, un erosion chamber and a recycling container, as shown in Fig (2). The experimental process is as follows: first, air compressors are used to provide a height-pressure airflow, and airflow control valves are used to control the erosion rate produced by this flow; second, the sandblasting gun is used to direct the sand flow from the sandbox and mix it with the height-pressure airflow into the erosion chamber; finally, the abraded sand particles are collected in the recycling container and recycled for use in other experiments. The comparison of the glass sample sprayed with zinc before and after erosion requires the accurate measurement of the mass of the sample before and after the experiment using a precision electronic balance. This section presents the analysis at the erosion velocity of sand and dust of 4 m/s. The selected abrasion angles are 15°, 30°, 45° and 60° to study the effect of sand and dust erosion on photovoltaic module and its performance parameters.

The erosion experiment was limited to 30 min because of the small size of the sand particles 90um used and the long time required for the erosion process of the coating layer by wind and sand [14].

2.2.2. Evaluation of Erosion Results

The degree of erosion damage to the PV module can be characterized by the relative erosion rate E_0 [20], which is expressed as shown in (1).

$$E_0 = m_1 - m_2 / m_1 \quad (1)$$

Where m_1: mas of sample before erosion.

m_2: mas of sample after erosion.

3. Results and Discussion

3.1. Relative Erosion Rate of ZnO in Relation to the Angle of Erosion.

Fig (3) illustrates how the sand particle impact angle affects the ZnO coating's degradation rate. The erosion rate rises steadily as the impact angle increases, from roughly 0.00164 mg/g at 15° to roughly 0.00220 mg/g at 60°. The gradual increase between 15° and 45° indicates that as the normal component of the impact force increases, the coating undergoes incremental surface degradation. Improved material erosion at greater impact angles is indicated by a more noticeable increase between 45° and 60°. This behavior is typical of brittle materials, where crack initiation and propagation rather than cutting or plowing mechanisms are the main factors controlling erosion. Higher impact angles cause the usual impact stress to take over, which encourages the development of lateral and radial cracks beneath the coating surface. Increased erosion loss and coating fragment spallation are the results of these cracks spreading and coalescing. The greatest erosion rate observed at 60° suggests that the degradation of the ZnO covering during sand-particle bombardment is mostly caused by normal impact pressures. This pattern implies that brittle fracture processes govern the erosion mechanism, resulting in increasing material erosion and progressive surface deterioration as the impact angle gets closer to normal incidence [14].

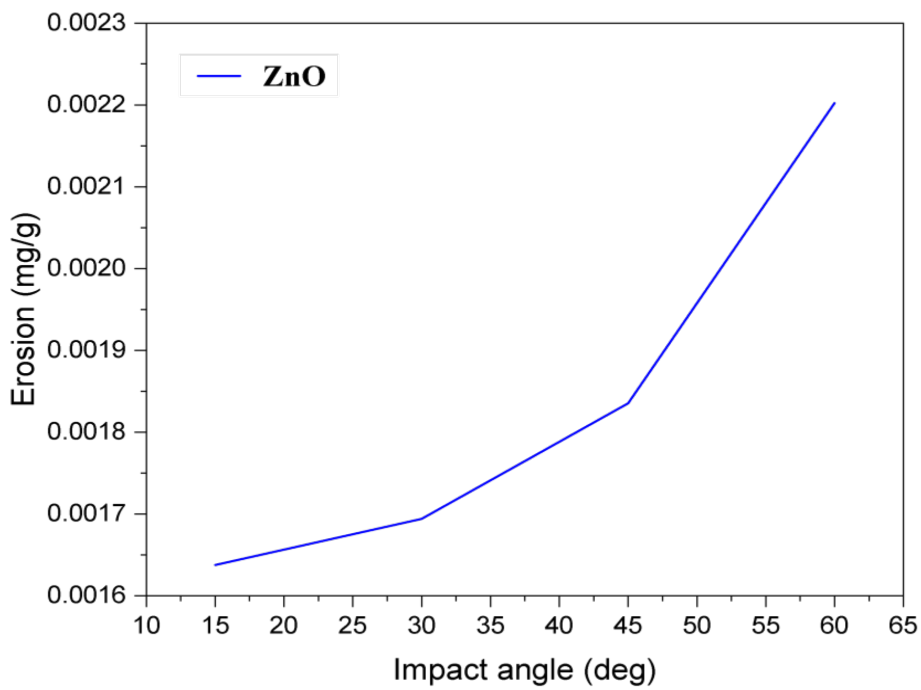

Fig. 3: The rate of erosion of the zinc oxide layer changes as a function of the angle of impact of the sand particles.

3.2. X-Ray Diffraction (XRD)

To identify the crystalline structure of ZnO films, XRD patterns were recorded in range 20-80 as shown in Fig (4). The diffractogram patterns were indexed properly for all crystalline peaks and compared with the JCPDS data files hexagonal wurtzite ZnO(card no. 036-1451). The diffraction peaks of ZnO NPs at (100), (002), (101), (102), (110), (103) (2 0 0), (1 1 2), and (2 0 1) which correspond to 2θ = 31.92°, 34.84°, 36.48°, 48.04°, 56.75°, 63.37°,66.87,68.42 and 69.62respectively. The diffraction peaks located at 2θ = 28.82,45.72 50.77and 59.32°corresponding to $Zn(OH)_2$ (PDF No 32-1469). While diffraction peak at 2θ = 40.02 indicate to Zn according to Card No. 004-0784.The average crystallite size of ZnO peaks was estimated by Scherer's formula was found to be (15.91) nm. It observed broad peaks and the average crystal size indicates the formation of nanocrystals with a high surface area that could be useful in photovoltaic applications [18-23].

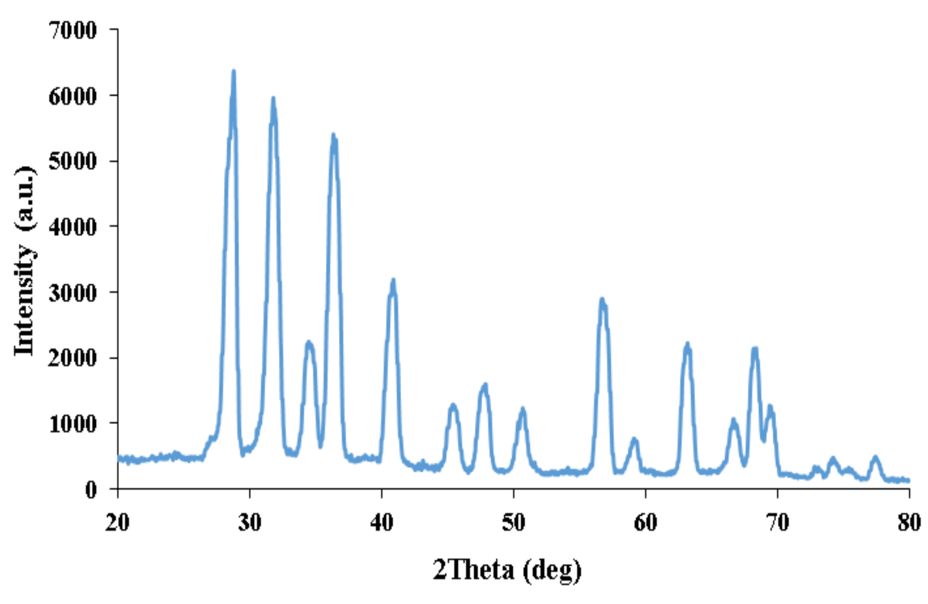

Fig. 4: XRD of ZnO film.

3.3. Ultraviolet-Visible (UV-VIS)

Fig (5) presents the measured absorption spectra of ZnO colloidal solution versus wavelength in the range (200-1100) nm. It was observed that the absorption is maximum in the UV- region (short wavelength – high photon energy) and decreases steeply with increasing wavelength. This behaviour is caused by the interaction of the incident photons with the material, where the photons with energies equal or greater than the optical band gap are absorbed and electrons are promoted from the valance band to the conduction band. At longer wavelengths there were lower absorption values because the probability of electronic transitions diminished as the photon energy decreased. ZnO have high transmittance in the VIS-IR spectrum, the highest transmittance recorded 86%, for ZnO at wavelength 400-1100 nm, this shows their potential used in photovoltaic devices [24].

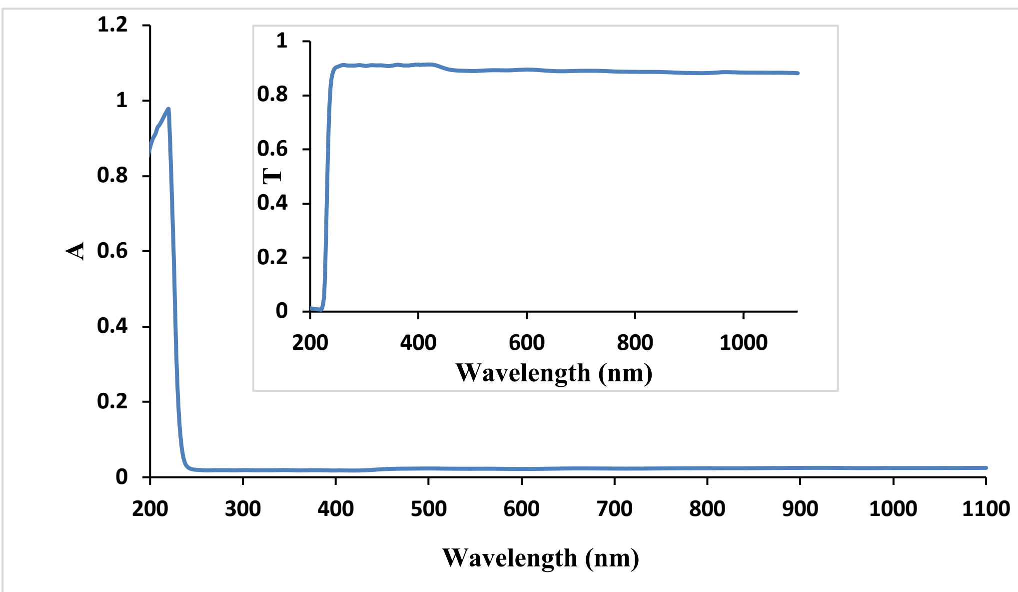

Fig. 5: Absorption and Transmittance spectra of ZnO film.

3.4. Atomic Force Microscopy (AFM)

Fig (6&7) display three - dimensional (3D) AFM images scanned over a surface area of 2 × 2 μm2 for the ZnO films before and after erosion. Fig (6) shows images of ZnO , it observed a uniform distribution and exhibits small spherical peak on the surface, with mean roughness 1.98 nm, RMS (3.08 nm) and mean grain size 51.96 nm respectively, these values indicate a relatively uniform surface composition with limited agglomeration of grains. While ZnO film observed change in surface morphology after erosion, this led to formation clear and large peaks as shown in Fig (7). Thus, the mean roughness increasing to5.6 nm, RMS to (7.04) nm and it is noted that the sample exhibited an apparent grain size rather than a true grain size after erosion, reaching approximately 121 nm. This increase is not attributed to actual grain growth; rather, it is most likely associated with the partial deterioration of the film and the removal of portions of the ZnO layer from the glass substrate during the erosion process. This phenomenon was clearly observed experimentally, as isolated agglomeration-like regions remained attached to the substrate surface. Consequently, during AFM analysis of the eroded sample, the software identified these isolated agglomerations or island-like structures as larger surface grains. The AFM image further confirms the significant change in surface morphology, showing the presence of large peaks on the surface. It is evident from the obtained results that both the average surface roughness and the root mean square roughness (RMS) increased after the erosion process. This increase can be attributed to the impact of sand particles striking the sample surface at high velocity, resulting in the removal of portions of the film and the formation of small pits and irregularities on the surface. In addition, grains that are weakly bonded to the surface tend to detach, whereas more strongly adhered grains remain protruding on the glass substrate. Since the erosion, process does not occur uniformly across the surface, pronounced peaks and valleys are generated, leading to an increase in both the surface roughness and RMS values. Abbott-Firestone curve shows that the sample before erosion has a smooth slope and relative gradient, indicating a homogeneous distribution of heights and a uniform loading surface. However, after erosion, the curve becomes wider and more disturbed, indicating a decrease in the effective loading area of the film. This is due to the partial removal of the ZnO film with some isolated areas on the substrate. This reduces the surface's ability to provide a uniform load-bearing distribution, and thus deep peaks and valleys are formed due to the sandblasting process. This confirms the increase in roughness and RMS.

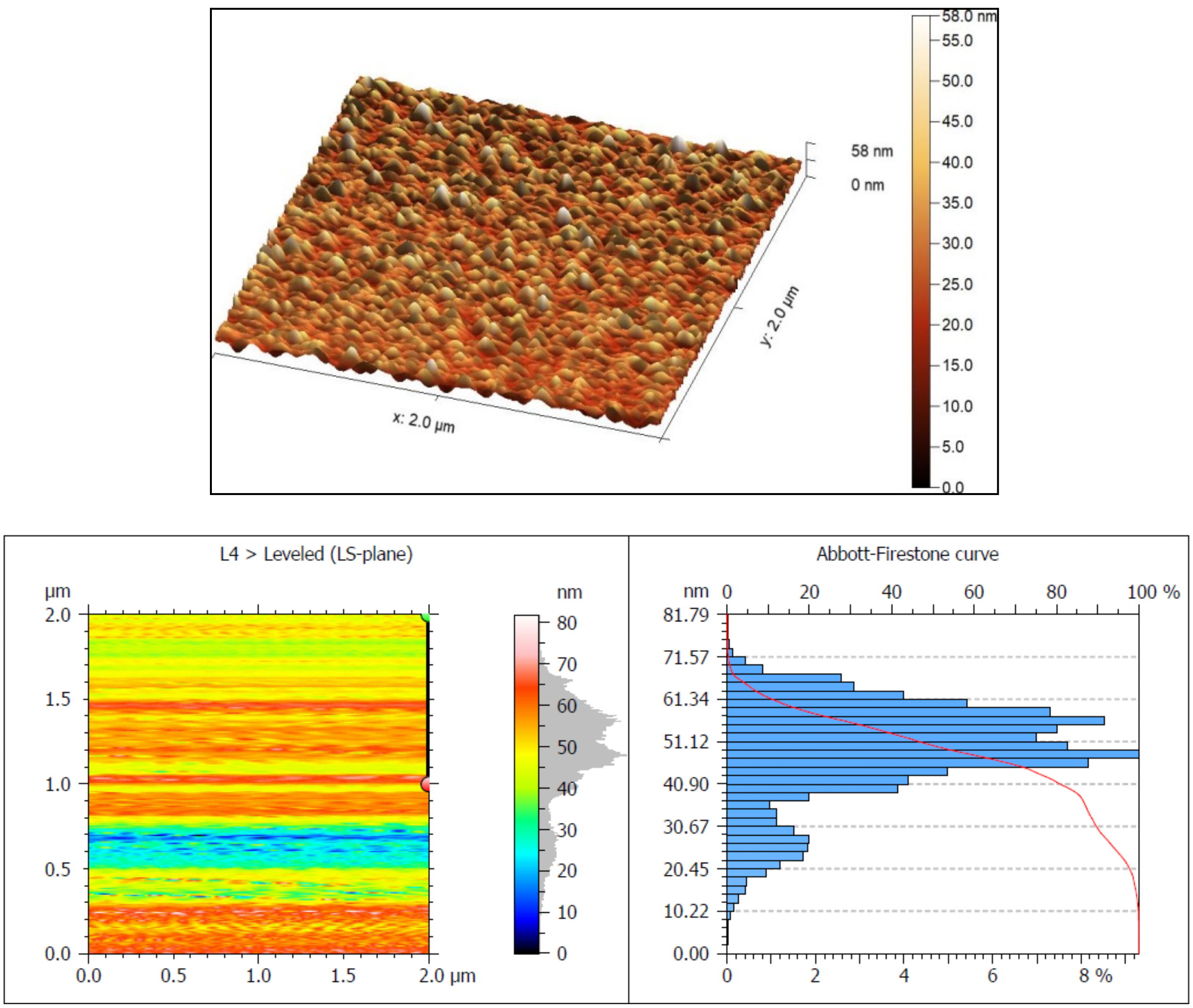

Fig. 6: 3D AMF Images and chart distribution for ZnO before erosion.

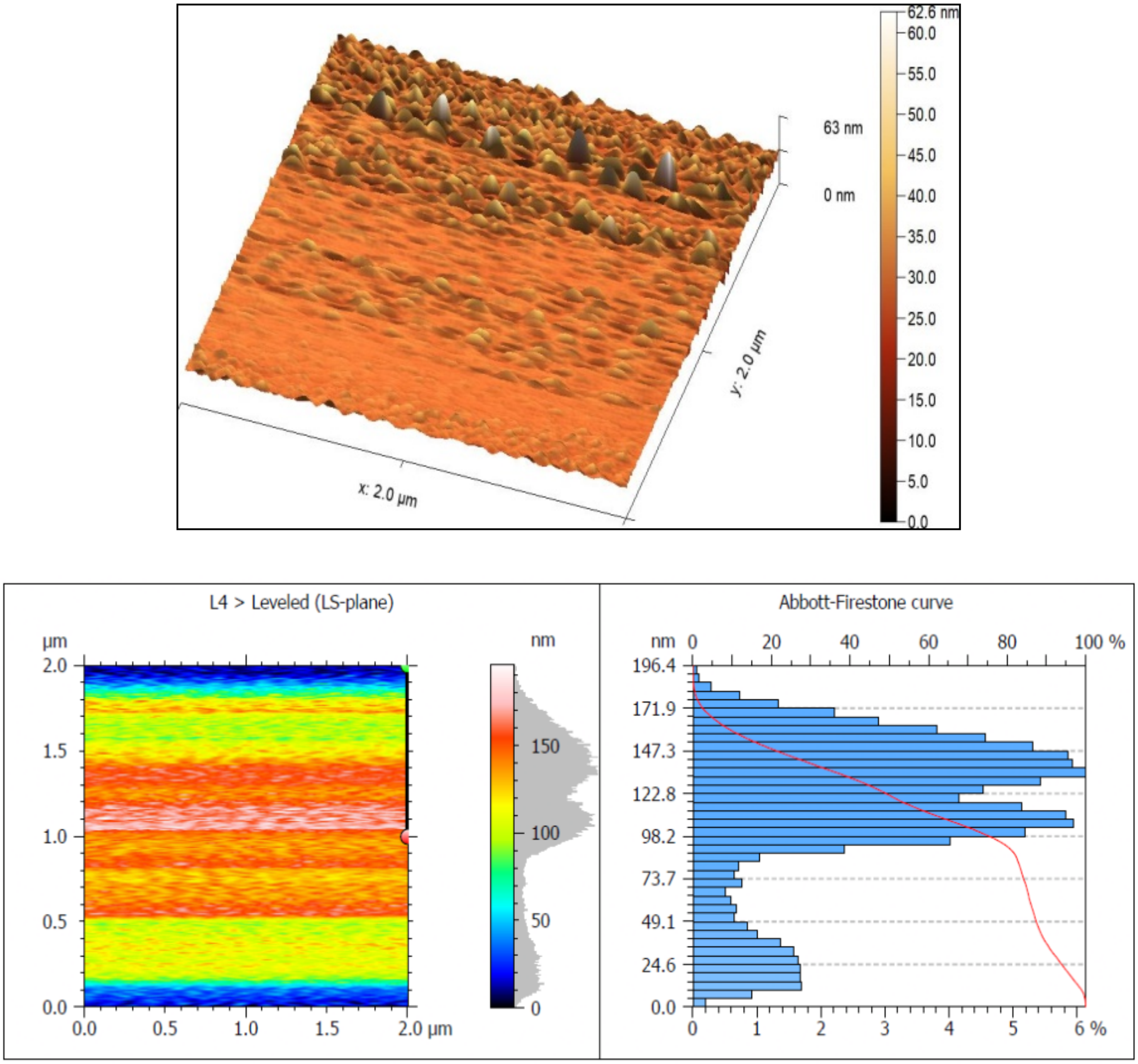

Fig. 7: 3D AMF Images and chart distribution for ZnO after erosion.

3.5. Scanning Electron Microscopy (SEM)

(Fig 8,a) shows the morphological characteristics of dissolved zinc oxide nanoparticles at a concentration of (0.1) M which is deposited on glass substrate (2.5 x 2.5) cm has different particles sizes. Clear differences in particle size can be observed from the images. The diameter of the zinc oxide nanoparticles is (50-200) nm. It consists of nanoparticles with various geometric shapes, such as spherical or silica-like forms. Visual features indicate the presence of closely packed, small grains, consistent with scanning electron microscopy (SEM) images of nanomaterials. This is particularly true for zinc oxide (ZnO) particles. The homogeneity and regularity of the film deposited on the glass indicate a suitable preparation and deposition method, resulting in surfaces with strong hardness and cohesion. There is no evidence of dislocations, cracks, or interstitial spaces, and the deposition temperature does not generate any defects in the film. This process aims to damage the coating to measure its strength. The test mechanism involves directing a high-pressure stream of sand or abrasive material at the film. The objective is to measure the force or pressure required to remove or peel the coating from the surface, reflecting the quality of the preparation. As shown in the figure, after sandblasting the zinc oxide film, a large surface area composed of nanoparticles is removed, and the remaining particles are fragmented into spherical or semi-spherical particles with dimensions not exceeding 70 nanometers, as illustrated in the (Fig 8,b) [25,26].

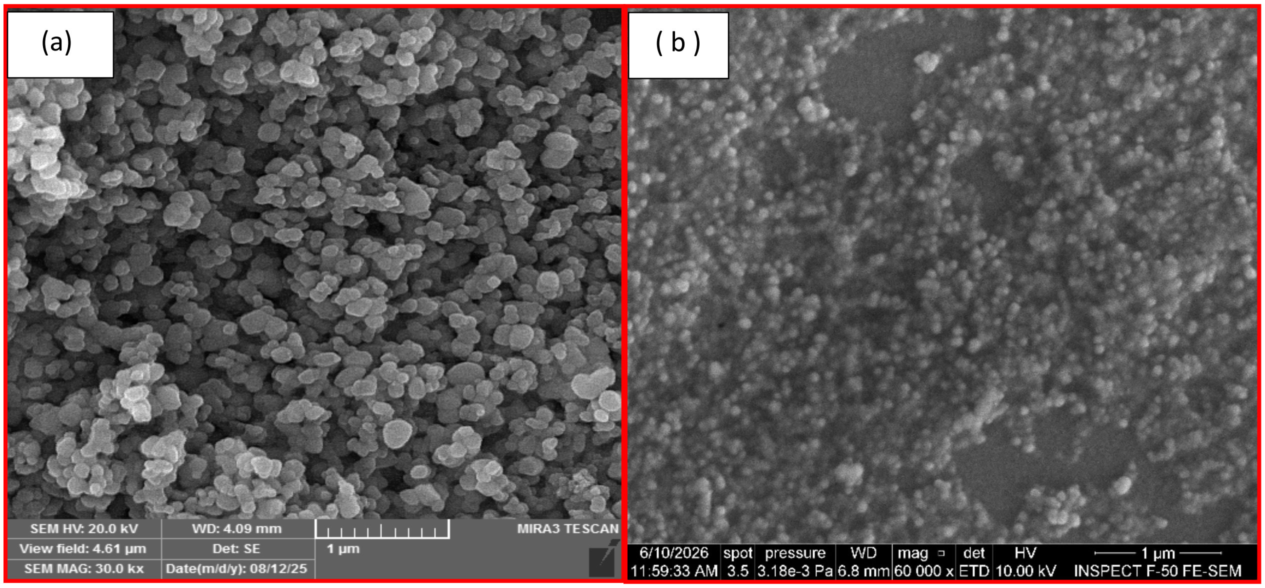

Fig. 8: (a) Image of ZnO film before erosion, (b) Image of ZnO film after erosion.

3.6. Energy Dispersive X-ray (EDX)

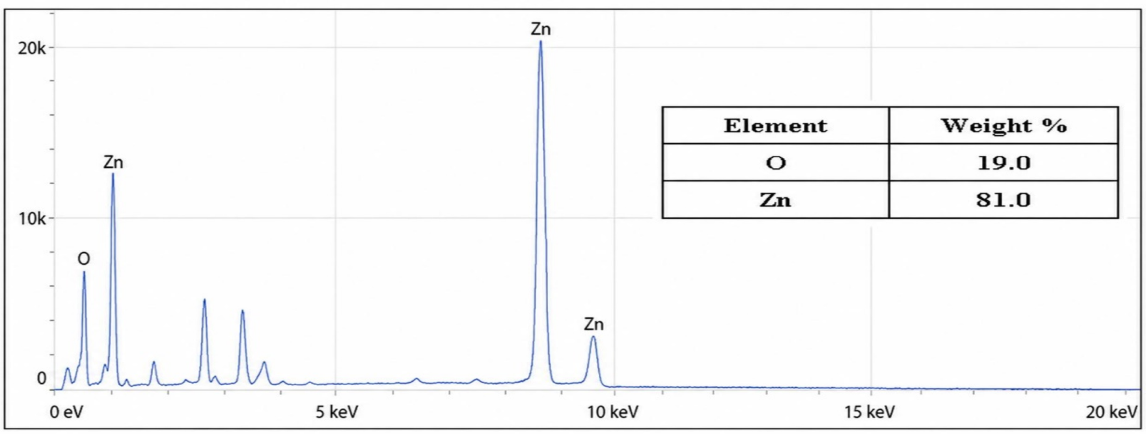

Fig. 9: EDX Spectra of Zinc Oxide film before erosion.

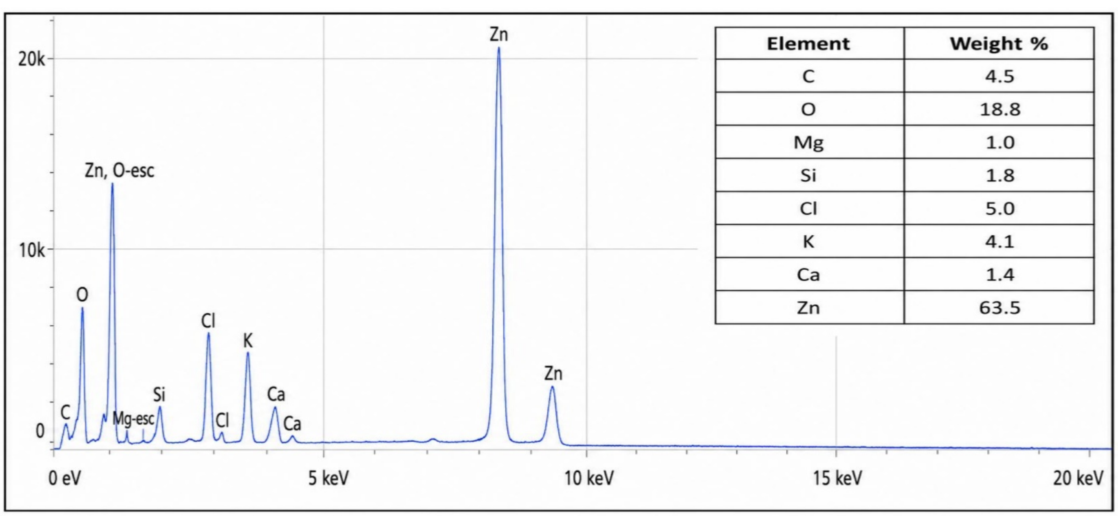

Fig. 10: EDX Spectra of Zinc Oxide film after erosion.

The graph in Fig (9) represents an energy-dispersive X-ray spectroscopy (EDS or EDX) spectrum, which is used to determine the elemental composition of a sample. The main features of the spectrum are: the x-axis (horizontal), representing the energy of the X-rays measured in kilo electron volts (keV); the y-axis (vertical), representing the intensity or counting rate of the detected X-rays; and the peaks, each sharp peak indicating a specific element present in the sample. The elements identified based on the markings in the spectrum are: peaks: Zinc (Zn): Forms a strong, characteristic line (k_α at 8.63 keV). It is noted as the predominant element in the sample. There is also a very sharp, elongated peak and a smaller secondary peak at other energy levels (k_β at 1.63 keV). Oxygen (O): Shows a distinct, noticeable peak at a lower energy level (near the left side of the graph).

The selected portion of the image in Fig (10) shows the energy-dispersive X-ray spectroscopy (EDX/EDS) spectrum of the zinc oxide film after sandblasting, based on the chemical composition and elemental ratios in the sample. As shown in the table accompanying the graph, the detected elements and their weight percentages are as follows: Zinc (Zn): The largest percentage at 63.5%, exhibiting distinct and high peaks in the spectrum at various energy levels (such as a sharp peak near 1 keV and a peak at approximately 8.6 keV). Oxygen (O): The second most abundant element at 18.8%, with its peak appearing near the beginning of the graph (around 0.5 keV), often indicating that the substance is an oxide (such as zinc oxide (ZnO)). Chlorine (Cl): 5.0%. Carbon (C): 4.5% (possibly due to the carbon tape used to stabilize the sample during testing). Potassium (K): 4.1%. Silicon (Si): 1.8% (likely from the substrate or impurities from erosion). Calcium (Ca): 1.4%. Magnesium (Mg): 1.0%. Axes: Horizontal axis (X-axis): Represents energy in kiloelectron volts (keV), with peaks appearing at specific energy values that characterize each chemical element. Vertical axis (Y-axis): Represents the intensity of the electromagnetic signal (number of pulses or radiations detected).

This work addresses modern concepts regarding the most significant detrimental effects impacting building walls and equipment, particularly solar cells. This comparison is with reference [27] which focused on studying the impact of seasonal variations on the performance of photovoltaic modules. This study, conducted at the University of Technology in Baghdad, Iraq, in 2023, evaluated a 3.3 kW grid-connected photovoltaic system. Environmental data, such as ambient temperature, solar radiation intensity, wind speed, humidity, and dust levels, were collected throughout the study period. Several system parameters were assessed, and this membrane is considered the optimal solution for mitigating all environmental losses.

4. Conclusion

ThiThis paper investigates the damage behavior and durability of Zinc Oxide (ZnO) coatings on the top glass of photovoltaic (PV) panels. The main research question was to determine the relationship between erosion and impact angles to understand the effect of erosive wear from windblown sand on the mechanical integrity and long-term performance of these protective films in arid environments. The results show an unambiguous agreement that ZnO coatings demonstrate brittle material behavior in solid particle erosion. The erosion rate gradually increases with the impact angle, from around 0.00164 mg/g at 15° to about 0.00220 mg/g at 60°. This suggests that degradation is mainly governed by normal impact forces which induce crack initiation, propagation and spallation of coating fragments. The coatings exhibit high optical transmittance (up to 86%) applicable for solar application. Nevertheless, destructive tests reveal the high-pressure sand streams lead to significant material erosion and particle fragmentation. However, these results leave several gaps for future study to resolve. The authors note that the available literature is skewed towards chemical precursors and photocatalytic performance, and not towards long-term mechanical robustness. One main bottleneck is the compromise between the high surface roughness needed to produce superhydrophobic “self-cleaning” properties and the optical transparency needed for PV efficiency. Moreover, more detailed information on the specific mechanisms by which the physical properties affect the particle motion and erosion is needed to ensure the long-term safe operation of solar plants in erosive desert environments.

References.

[1] M. L. Adekanbi, E. S. Alaba, T. J. John, T. D. Tundealao, and T. I. Banji, "Soiling loss in solar systems: A review of its effect on solar energy efficiency and mitigation techniques," *Cleaner Energy Systems*, vol. 7, p. 100094, 2024.

[2] J. Alqallaf, N. Ali, J. A. Teixeira, and A. Addali, "Solid Particle Erosion Behaviour and Protective Coatings for Gas Turbine Compressor Blades—A Review," *Processes*, vol. 8, no. 8, p. 984, 2020.

[3] V. Bonu and H. C. Barshilia, "High-Temperature Solid Particle Erosion of Aerospace Components: Its Mitigation Using Advanced Nanostructured Coating Technologies," *Coatings*, vol. 12, no. 12, p. 1979, 2022.

[4] C. Cheng, A. Amini, C. Zhu, Z. Xu, H. Song, and N. Wang, "Enhanced photocatalytic performance of TiO2-ZnO hybrid nanostructures," *Scientific Reports*, vol. 4, p. 4181, 2014.

[5] H. McI. Clark, "Impact angle, particle energy and mass loss in erosion by dilute slurries," *Wear*, vol. 150, pp. 217–230, 1991.

[6] COMSOL Multiphysics, "Solar Panel in Periodic Flow," *CFD Module Application Library*, 2023.

[7] I. El-Mahallawi et al., "Solar PV Panels-Self-Cleaning Coating Material for Egyptian Climatic Conditions," *Sustainability*, vol. 14, no. 17, p. 11001, 2022.

[8] E. H. M. Fares, "Enhancing the Performance of Photovoltaic (PV) Panels Using Anti-Soiling Coatings Techniques," Ph.D. dissertation, Hamad Bin Khalifa University, Doha, Qatar, 2022.

[9] I. Finnie, "Erosion of surfaces by solid particles," *Wear*, vol. 3, no. 2, pp. 87–103, 1960.

[10] A. Franco and S. G. Roberts, "The effect of impact angle on the erosion rate of polycrystalline α-Al2O3," *Journal of the European Ceramics Society*, vol. 16, no. 12, pp. 1365–1375, 1996.

[11] S. Guo et al., "A ZnO-TiO2-Amygdalin nanocomposite for bone regeneration and antimicrobial activity," *Scientific Reports*, vol. 15, no. 1, 2025.

[12] I. Hussainova, "Assessment of cermets performance in erosive media," *Encyclopedia*, vol. 3, 2023.

[13] A. C. Karaoglanli, K. M. Doleker, and B. Demirel, "Solid particle erosion behavior of thermal barrier coatings produced by atmospheric plasma spray technique," *Selcuk University Scientific Research Projects*, 2015.

[14] X. Liu, N. Wang, M. Zhao, and X. Hu, "Experimental Study on the Effect of Sand and Dust on the Performance of Photovoltaic Modules in Desert Areas," *Energies*, vol. 17, no. 3, p. 682, 2024.

[15] X. Liu et al., "Mechanism underlying the effect of physical properties on the dynamic behaviours and erosion characteristics of particles on solar photovoltaic panels," *Journal of Materials Science*, 2023.

[16] A. Naji, "Study and analysis of the damage behavior of coatings materials like (ZnO) on the top glass of pv panels," [Research Background and Introduction], 2026.

[17] Y. I. Oka, S. Mihara, and T. Yoshida, "Impact-angle dependence and estimation of erosion damage to ceramic materials caused by solid particle impact," *Wear*, vol. 267, no. 1-4, pp. 129–135, 2009.

[18] V.N. Kalpanaa, Bala Anoop Sirish Katarua, N. Sravania, T. Vigneshwaria, A. Panneerselvamb, V. Devi Rajeswar .Biosynthesis of zinc oxide nanoparticles using culture filtrates of Aspergillus niger: Antimicrobial textiles and dye degradation studies. OpenNano 3 (2018) 48–55

[19] Biosynthesis of ZnO Nanoparticles Using the Aqueous Extract of Mucuna pruriens (utilis): Structural Characterization, and the Anticancer and Antioxidant Activities Nozipho P. Gamedze1 • Doctor M. N. Mthiyane1,2 • Sydney Mavengahama2,3 • Moganavelli Singh4 • Damian C. Onwudiwe5,6. Chemistry Africa (2024) 7:219–228. https://doi.org/10.1007/s42250-023-00750-z

[20] Dionisio da Silva Birona,b*, Venina dos Santosb , Carlos Pérez Bergmanna .Synthesis and Characterization of Zinc Oxide Obtained by Combining Zinc Nitrate with Sodium Hydroxide in Polyol Medium. Materials Research. 2020; 23(2): e20200080 . DOI: https://doi.org/10.1590/1980-5373-MR-2020-0080

[21] M. Ghaedi a, H. Zare Khafri a, A. Asfaram a, A. Goudarzi Response surface methodology approach for optimization of adsorption of Janus Green B from aqueous solution onto ZnO/Zn(OH)2-NP-AC: Kinetic and isotherm study. Spectrochimica Acta Part A: Molecular and Biomolecular Spectroscopy Volume 152, 5 January 2016, Pages 233-240

[22] Jia-kui Song Æ Ming-bo Zheng Æ Zhen-jiang Yang Æ Hui-qin Chen Æ Hai-yan Wang Æ Jin-song Liu Æ Guang-bin Ji Æ Hai-qian Zhang Æ Jie-ming Cao .Synthesis of Novel Flower-Like Zn(OH)F via a Microwave- Assisted Ionic Liquid Route and Transformation into Nanoporous ZnO by Heat Treatment. Nanoscale Res Lett (2009) 4:1512–1516 DOI 10.1007/s11671-009-9428-1

[23] Abrar A. Khan1 & M. Mumtaz1 & Mubasher1 & M. Khan1 & Liaqat Ali1 & M. Rahim1 & M. Ali . Effects of Non-magnetic Metallic Zinc Nanoparticles on the Dielectric Properties of CuTl-1223 Superconducting Phase. J Supercond Nov Magn 34, 1341–1350 (2021). https://doi.org/10.1007/s10948-021-05862-6

[24] Yehezkiel Steven Kurniawan1, Leny Yuliati1,2,*) Activity Enhancement of P25 Titanium Dioxide by Zinc Oxide for Photocatalytic Phenol Degradation .Bulletin of Chemical Reaction Engineering & Catalysis, 16 (2) 2021, 310-319

[25] Shakeel, N.; Piwoński, I.; Iqbal, P.; Kisielewska, A. Green Synthesis of titanium dioxide nanoparticles: Physicochemical characterization and applications: A review. Int. J. Mol. Sci. 2025, 26, 5454. [Google Scholar]

[26] Thakur, B.K.; Kumar, A.; Kumar, D. Green synthesis of titanium dioxide nanoparticles using azadirachta indica leaf extract and evaluation of their antibacterial activity. S. Afr. J. Bot. 2019, 124, 223–22.

[27] Abd, A.O., Al-Nasser, T.M.A., Ekaab, N.S., Alawee, W.H., Kazem, H.A. and Chaichan, M.T. 'Experimental Evaluation of Climate Parameters Impact on Grid-Connected PV Electricity Generation: A Practical Approach', Journal of Engineering Science and Technology, Special Issue on ICSSD 2023, pp. 288–306.